Article

In Vitro Assessment of the Impact of Ultraviolet B Radiation on Oral Healthy and Tumor Cells

Otilia Gag [1], Ioana Macasoi [2,3,*], Iulia Pinzaru [2,3], Stefania Dinu [1,4], Ramona Popovici [1], Mioara-Raluca Cosoroaba [1], Roxana Buzatu [1], Madalina Cabuta [2,3] and Sorin Dan Chiriac [5]

[1] Faculty of Dental Medicine, "Victor Babeş" University of Medicine and Pharmacy, 9 Revolutiei 1989 Ave., 300070 Timisoara, Romania

[2] Faculty of Pharmacy, "Victor Babes" University of Medicine and Pharmacy Timisoara, Eftimie Murgu Square No. 2, 300041 Timisoara, Romania

[3] Research Center for Pharmaco-Toxicological Evaluations, Faculty of Pharmacy, "Victor Babes" University of Medicine and Pharmacy Timisoara, Eftimie Murgu Square No. 2, 300041 Timisoara, Romania

[4] Pediatric Dentistry Research Center, Faculty of Dental Medicine, "Victor Babes" University of Medicine and Pharmacy Timisoara, 9 Revolutiei 1989 Ave., 300070 Timisoara, Romania

[5] Faculty of Medicine, "Victor Babes" University of Medicine and Pharmacy Timisoara, Eftimie Murgu Square No. 2, 300041 Timisoara, Romania

* Correspondence: macasoi.ioana@umft.ro

Abstract: Ultraviolet radiation (UVR) is generally considered a primary tumorigenic agent. While UVR exposure has been studied, especially at the skin level, the impact of UV exposure on internal tissues and its effect on the appearance and the development of tumors has not yet been fully examined. Although there are maximum limits for UVR exposure on external tissues, other internal tissues, such as oral tissue, can be exposed to UVR as well. Over the course of diagnosis and treatment, oral cells may be exposed to ultraviolet radiation; however, there has not been an established limit for UV radiation exposure. Therefore, the aim of the current study was to examine the effects of ultraviolet-B (UVB) radiation at two doses (2.5 and 5 J/cm^2) on tumor cells (pharyngeal carcinoma and tongue carcinoma) and healthy cells (gingival fibroblasts). The viability of the cells and their morphology, actin filaments, and nuclei structures; the expression of anti-apoptotic (Bcl-2) and pro-apoptotic (Bax) genes; and the roles of caspases-3/7, 8, and 9 were determined after the cells had been exposed to UVB. The experiments revealed that both types of cell lines showed reductions in viability, especially at a dose of 5 J/cm^2. Additionally, apoptotic-like changes (rounding of the cells, the condensation of the nuclei, the re-organization of the actin filaments) were observed in all analyzed cells. The expression of anti-apoptotic (Bcl-2) and pro-apoptotic (Bax) genes revealed that UVB (5 J/cm^2) may induce apoptosis in both oral tumor and healthy cells. Moreover, an analysis of caspases-3/7, 8, and 9 showed that UVB exposure enhanced their activity, suggesting that cell death could be caused by both intrinsic and extrinsic apoptosis. Accordingly, UVB exposure at the maximum doses used in dental practices (5 J/cm^2) induced nonselective apoptotic changes, thereby reducing both tumor and healthy cell viability.

Keywords: ultraviolet-B radiation; cell viability; cell morphology; oral cancer; RT-PCR

1. Introduction

Ultraviolet radiation (UVR) is known to play a major role in tumor formation [1]. In addition to DNA damage, immunosuppression, and mutagenesis, UVR can also interfere with various types of viruses, such as human papillomavirus (HPV), resulting in carcinogenesis [2]. According to their wavelengths, UVR can be divided into three subtypes: UVA (320–400 nm), UVB (280–320 nm), and UVC (200–280 nm) [3]. Among these, UVC radiation is largely filtered by the ozone layer, while between 90 and 99% of UVA and between 1 and 10% of UVB radiation reaches the earth's surface. Nevertheless, UVB is the most implicated

type of UVR in carcinogenesis, so exposure to UVB is the most relevant clinical form from the perspective of tumor initiation [4]. UVR has been recognized as a human carcinogen since 2009 by the World Health Organization, who has set threshold limit values for safe UV exposure of skin and eye tissues [5]. As of now, however, internal tissues, including oral tissues, do not have a threshold limit. As UV radiation is used in the medical and dental fields on a large scale, it is crucial to understand how UVR affects internal tissues in terms of carcinogenicity. The epigenetic changes play a key role in the development of tumors. Despite this, there has been limited information on the effect of UV radiation on the inhibition of tumor suppressor genes that lead to skin cancer. The UV exposure of the skin has also been associated with epigenetic alterations, such as changes in DNA methylation and DNA methyltransferases [6]. The most studied epigenetic modification has been DNA methylation, since a direct correlation was demonstrated between ultraviolet exposure and epidermal methylation profiles [7]. Moreover, DNA damage as a result of UV exposure has been demonstrated to initiate various cell recovery mechanisms, as well as cell-cycle arrest and apoptosis [8]. Furthermore, epigenetic changes caused by ultraviolet exposure have been studied primarily at the skin level. The results of a more recent study showed that normal human dermal papilla cells were affected by UVB exposure, causing alterations to the microRNA profiles associated with cell survival and death [9].

The exposure to ultraviolet radiation is one of the most significant risk factors for skin cancer [10]. There is, however, the possibility that other tissues, such as the oral tissues, can also be affected by UV radiation, both internally and externally. In most cases, oral tissues are exposed to UVR indoors during various dental diagnostic and treatment procedures [11–13]. The medical causes of exposure to UVR are supplemented by other factors, including exposure to fluorescent lamps and quartz halogen bulbs [14]. The greatest exposure of the oral cavity to UVR has been observed with the use of tanning devices that emit large quantities of both UVA and UVB light [15]. There is also some evidence that certain teeth whitening procedures use UVR; however, the effectiveness of these procedures has been controversial [16].

Multiple UV applications in current medical practice include for the disinfection and decontamination of surfaces and water; for the detection of various toxic substances; in protein analysis and medical imaging; for strengthening polymers, and ineffective light therapy for various skin pathologies [17–22]. A wide range of dental applications benefit from ultraviolet radiation. For example, composite resin restorations are often difficult to observe visually, which presents difficulties when replacing them. The use of UV light in this case can be useful to determine whether the composite resin has been completely removed [11]. UVB has also proved effective in dental practice for disinfecting the root canals in conjunction with sodium hypochlorite. When using ultraviolet light at 254 nm and 300 mJ/cm^2, a significantly improved antibacterial effect was obtained, as compared to sodium hypochlorite alone [23]. Furthermore, UVB, applied at doses of up to 558 mJ/cm^2, was found to have bactericidal effects on oral bacteria, including the bacteria associated with caries and apical periodontitis [24].

Oral cancer is considered a pathological neoplasia found in the oral cavity (lips, tongue, cheeks, pharynx). Approximately 90% of oral cavity malignancies are squamous cell carcinomas. Oropharyngeal cancer, which can affect even the tongue, is the most common type of oral cancer, and if it is not detected in time, it can pose a major risk to survival [25]. Aside from this, oropharyngeal cancer adversely affects the quality of life of patients, since it interferes with daily activities, such as eating and speaking [26]. It is estimated that over 500,000 patients worldwide are diagnosed with various forms of oral cancer and that more than half die within 5 years of their diagnosis [27]. The observations from epidemiological studies have indicated that low- and middle-income countries have the highest incident rate of oral cancer. The reason for this was that patients from these countries were more likely to be exposed to risk factors, such as smoking and alcohol consumption [28]. Aside from these well-known risk factors, UV radiation has proven to be a significant contributor to the development of oral cancer. As a mechanism by

which UVR contributes to tumorigenesis, it alters the DNA of several structures of the oral cavity; furthermore, it may also activate HPV, which then releases anti-apoptotic factors that prevent mutant cells from dying and, thus, increase their carcinogenic potential [29].

Based on these assumptions, the present study sought to examine the impact of UVB on pharyngeal carcinoma cells (Detroit-562) and tongue carcinoma cells (SCC4) and, in parallel, the effect on healthy gingival fibroblast cells (HGF). Therefore, the viability of tumor and healthy cells were assessed immediately after UVB exposure, and the effect on the nuclei and cytoskeleton structures were analyzed. In addition, a quantitative analysis of the markers implicated in the cellular apoptosis process (Bcl-2—anti-apoptotic protein and Bax—pro-apoptotic protein) was carried out to reveal the potential biological mechanisms involved in the changes produced after UVB exposure. Additionally, to deepen the mechanism of UVB-induced cell death, the caspases-3/7, 8, and 9 were quantified.

2. Materials and Methods

2.1. Reagents

In the present study, we used a series of reagents and supplements for the culture of cell lines, as follows: phosphate saline buffer (PBS), trypsin–EDTA solution, dimethyl-sulfoxide (DMSO), fetal calf serum (FCS), penicillin–streptomycin, hydrocortisone 21-hemisuccinate sodium salt, and MTT [3-(4,5dimethylthiazol-2-yl)-2,5-diphenyltetrazolium bromide] reagent acquired from Sigma Aldrich, Merck KgaA (Darmstadt, Germany). Fibroblast Basal Medium (ATCC® PCS-201-030™), Fibroblast Growth Kit-Low Serum (ATCC® PCS-201-041™), Eagle's Minimum Essential Medium (EMEM—ATCC® 30-2003TM), and Dulbecco's Modified Eagle's Medium/Nutrient Mixture F-12 Ham (DMEM: F-12, ATCC® 30-2006™) were purchased from ATCC (American Type Culture Collection, Lomianki, Poland). Rhodamine phalloidin (00027) was purchased from Biotium (Hayward, CA, USA) and DAPI (D9542—10 mg) from Sigma Aldrich, Merck KgaA (Darmstadt, Germany). Caspase-Glo(R) 3/7 Assay (G8090), Caspase-Glo(R) 8 Assay (G8200), and Caspase-Glo(R) 9 Assay (G8210) were purchased from Promega Corporation (Madison, WI, USA).

2.2. Cell Culture

In vitro studies were conducted using Detroit-562 (CCL-138TM), SCC4 (CRL-1624TM) and HGF (PCS-201-018™) cell lines obtained from the American Type Culture Collection (ATCC, LGC Standards GmbH, Wesel, Germany). The cells were cultured in a specific culture medium: EMEM in the case of Detroit-562 cells, DMEM:F-12 for SCC4 cells, and fibroblast basal medium for HGF cells. The media were supplemented with 10% fetal bovine serum and 1% antibiotic mixture (100 U/mL penicillin/100 μg/mL streptomycin). In addition, the specific medium for SCC4 cells, DMEM-F12, was supplemented with 400 ng/mL hydrocortisone, and the specific medium for HGF was completed with Fibroblast Growth Kit-Low Serum. The cells were maintained at a standard temperature (37 °C) and 5% CO_2.

2.3. UVB Exposure

The cells were cultured in 12-well plates at a density of 1×10^5 cells-per-well, for exposure to UVB. Every experiment was carried out on two plates: one plate exposed to UVB, and one plate was maintained at standard lighting and temperature conditions. Once the cells reached a confluence of approximately 90%, they were washed with PBS once, and then 1 mL of PBS was added in each well. In the following step, the cells were subjected to UVB treatment, while the control cells (also maintained in PBS) were kept out of the light. To eliminate possible interference between the medium and UVB, the medium was replaced with PBS before exposure to UVB. Therefore, the cells were exposed to UVB, at 312 nm and 2.933 mW/cm^2, resulting in total doses of 2.5 and 5 J/cm^2, respectively, at 14 and 28 min, respectively, using Biospectra system (Vilber Lourmat, France). The distance between the UVB source and the exposed cells was 20 cm.

2.4. Cell Viability Assessment

The MTT method was used to evaluate the impact of UVB radiation on the viability of pharyngeal carcinoma cells, tongue carcinoma cells, and gingival fibroblast cells. For this purpose, the cells were cultured in 96-well plates (1×10^4 cells-per-well). After reaching a confluence of approximately 90%, the cells were washed with PBS once, after which a volume of 200 μL/well of PBS was added, and the cells were exposed to UVB (2.5 and 5 J/cm^2). Immediately after exposure, PBS was replaced with 100 μL of fresh culture medium, 10 μL of MTT reagent was added to each well, and the plates were incubated for 3 h. Then, 100 μL/well of solubilization solution was applied, and the plates were kept at room temperature for 30 min. As a final step, the absorbance was measured at 2 wavelengths (570 and 630 nm) using the Cytation 5 apparatus (BioTek Instruments Inc., Winooski, VT, USA).

2.5. Cellular Morphology

A microscopic evaluation of the impact of UVB on cell morphology was conducted by photographing cells under bright field illumination. The images were captured with an Olympus IX73 inverted microscope equipped with a DP74 photo camera and analyzed using the CellSens V1.15 software (Olympus, Tokyo, Japan). Pictures were taken of both UVB-exposed cells and the control cells, which had not undergone UVB exposure.

2.6. Identification of the Nuclear Structure and Actin Filaments

The effects of UVB exposure on the nuclei and actin fibers were investigated using fluorescence immunocytochemistry. Therefore, exposed cells and control cells were washed with PBS and fixed with paraformaldehyde at 4 °C for 30 min. The next step was the permeabilization of the cell membrane with a solution of 2% Triton X-100/1 × PBS, followed by the blocking step of the permeabilization solution using a mixture of 30% FCS/0.01% Triton X-100. To visualize the actin fibers, cells were incubated for 20 min with rhodamine phalloidin (00027) from Biotium (Hayward, CA, USA), and for the visualization of the nuclei, cells were incubated for 15 min with 4,6-diamidino -2-phenylindole (DAPI) reagent. The images were captured using an Olympus IX73 inverted microscope provided with a DP74 camera photo and analyzed with CellSens V1.15 software (Olympus, Tokyo, Japan) and ImageJ software V1.53T (NHI, Bethesda, MD, USA; http://rsbweb.nih.gov/ij/, accessed on 10 February 2023). Apoptosis was quantified by using the apoptotic index calculated according to the formula below:

$$\text{Apoptotic index (AI) (\%)} = \frac{\textit{Number of apoptotic cells}}{\textit{Total number of cells}} \times 100$$

The nuclear morphology was evaluated using ImageJ software in accordance with procedures previously described in the literature [30].

2.7. Expression of Bcl-2 and Bax Genes

In order to comprehend the impact of UVB on the expression of genes involved in cellular apoptosis, the real-time reverse transcription–polymerase chain reaction (RT-PCR) assay was applied. In this study, Bcl-2 and Bax genes were studied (Thermo Fisher Scientific, Inc., Waltham, MA, USA). Consequently, the cells were cultured in six-well plates. To expose the cells to UVB, the cells were washed with PBS after reaching a confluence of approximately 90%, then a volume of 3 mL of PBS/well was added, and the cells were exposed to UVB (2.5 and 5 J/cm^2). A DS-11 spectrophotometer (DeNovix, Wilmington, DE, USA) was used to determine the amount of RNA immediately after exposure using a Trizol reagent and the Quick-RNA TM purification kit. Finally, RNA was produced using the Maxima$^®$ First Strand cDNA Synthesis Kit, and RT-PCR quantification was performed using the Quant Studio 5 real-time PCR system (Thermo Fisher Scientific, Inc., Waltham, MA, USA) in the presence of Power SYBR-Green PCR Master Mix.

2.8. Caspase Activity

Caspases 3/7, 8, and 9 activity were measured after exposure to UVB using the Caspase-Glo kit (Promega, Madison USA). The exposed and control cells were allowed to equilibrate at room temperature for 30 min after UVB exposure. Thereafter, 100 μL of Caspase-Glo reagent was added to each well and was followed by the plates being shaken for 30 s using a plate shaker, which ensured the homogenization of the well contents. Afterwards, the plates were incubated at room temperature for two hours. The measurement of luminescence was carried out by using the Cytation 5 instrument (BioTek Instruments Inc., Winooski, VT, USA).

2.9. Statistical Analysis

Results of the study were expressed as standard deviations ($\pm$SD). To compare the differences between the non-exposed and exposed groups, a one-way ANOVA test was applied, followed by Dunnett's multiple comparison post hoc test. The software used was GraphPad Prism, version 9.3.1 for Windows (GraphPad Software, San Diego, CA, USA, www.graphpad.com, accessed on 10 February 2023). Statistically significant differences between data were labeled with * (* $p < 0.05$, ** $p < 0.01$, and *** $p < 0.001$; **** $p < 0.0001$).

3. Results

3.1. Cell Viability and Morphology Assessment

Immediately following exposure to UVB, the Detroit-562, SCC4, and HGF cells were assessed for their viability using the MTT method.

As a result of exposure to UVB at a dose of 2.5 J/cm^2, both the pharyngeal carcinoma and tongue carcinoma cells showed a similar decrease in their viability of approximately 66% and 65%, respectively. Furthermore, healthy gingival fibroblast cells showed a decrease in the percentage of viable cells, although the decrease was not as pronounced as that observed in tumor cells (approximately 81%, Figure 1A). Furthermore, at the level of cell morphology, the Detroit and SCC4 cells were also found to exhibit morphological changes, as compared to control cells. Consequently, in this case, the cells became round and detached from the plate, resulting in a lower number of cells compared to cells not exposed to UVB. Healthy cells also underwent morphological changes, such as rounding of the cell shape and a decrease in confluency, but these changes were less pronounced than those of tumor cells (Figure 1B).

After exposure to UVB at a dose of 5 J/cm^2, it was found that tumor cells (Detroit-562 and SCC4) showed a significant loss in viability, with a value of approximately 66% and 56%, respectively, as compared to the controls, which had not been exposed to UVB. Exposure to UVB, however, had the greatest impact on healthy gingival fibroblast cells. Consequently, in this case, the viability was roughly 45%, as compared to the control cells (Figure 2A).

An evaluation of the cell morphology was performed in order to better understand the effects of UVB radiation on the pharyngeal and tongue squamous-cell carcinoma cells. It was observed that the morphology of the Detroit-562 cells did not change in the absence of UVB exposure, as the confluence and shape of the cells were similar to that of the cells before UVB exposure. The cells exposed to UVB, on the other hand, underwent changes in their morphology, becoming round with decreasing confluency (Figure 2B).
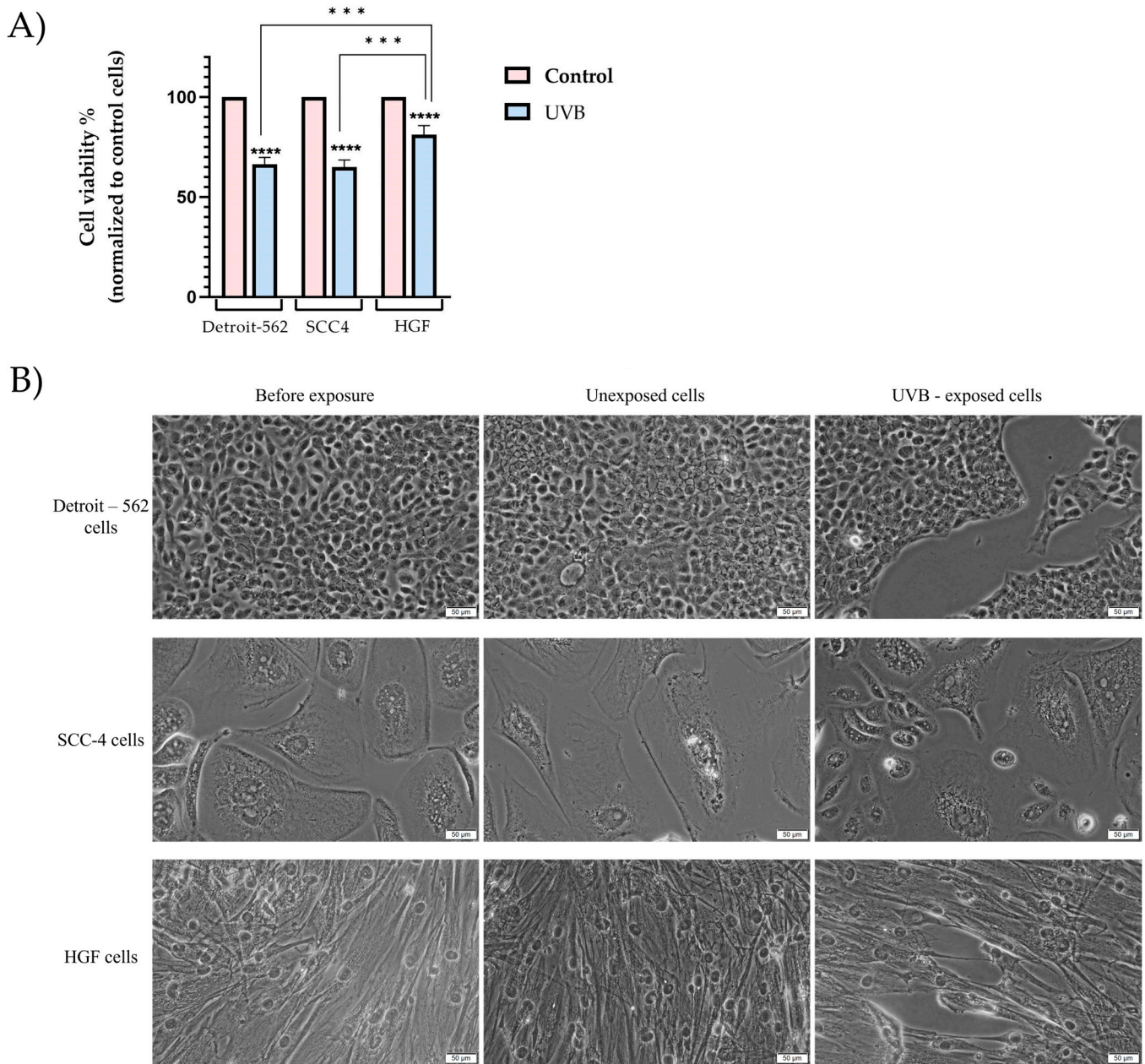
Figure 1. (**A**) In vitro assessment of the influence of UVB (2.5 J/cm^2) on the viability of Detroit-562, SCC4, and HGF cells. The MTT assay was performed immediately after UVB exposure. Data are presented as viability percentages (%) normalized to control (unexposed cells) and expressed as mean values ± SD in the three independent experiments performed in triplicate. The statistical differences between the control and the UV-irradiated groups were verified by applying a one-way ANOVA analysis followed by Dunnett's multiple comparisons post hoc test, and the difference between the responses of each cell line was verified by applying a one-way ANOVA analysis followed by a Tukey's multiple comparison post hoc test (*** $p < 0.001$; **** $p < 0.0001$); (**B**) in vitro morphological changes of Detroit-562, SCC4, and HGF cells before and after exposure to UVB. The scale bar indicates 50 μm.
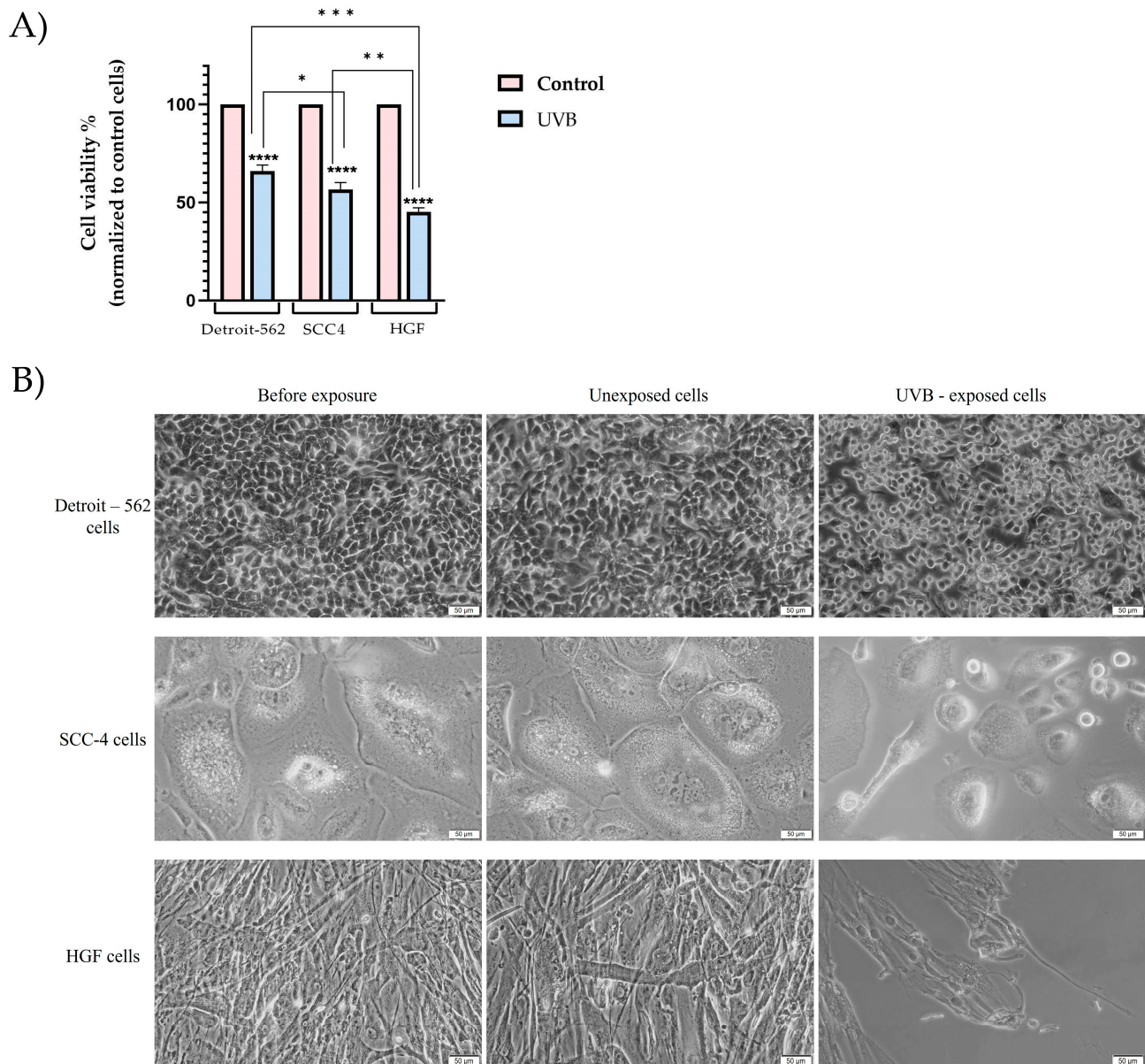
Figure 2. (**A**) In vitro assessment of the influence of UVB (5 J/cm^2) on the viability of Detroit-562, SCC4, and HGF cells. The MTT assay was performed immediately after UVB exposure. Data are presented as viability percentages (%) normalized to control (unexposed cells) and expressed as mean values $\pm$ SD of three independent experiments performed in triplicate. The statistical differences between the control and UV-irradiated groups were verified by applying a one-way ANOVA analysis followed by Dunnett's multiple comparison post hoc test and the difference between the responses of each cell line was verified by applying a one-way ANOVA analysis followed by Tukey's multiple comparison post hoc test (* $p < 0.05$; ** $p < 0.01$ and *** $p < 0.001$; **** $p < 0.0001$); (**B**) in vitro morphological changes of Detroit-562, SCC4, and HGF cells before and after exposure to UVB. The scale bar indicates 50 μm.

In the case of the SCC4 cells, similar changes were observed. As a result of exposure to UVB, the squamous cell carcinomas of the tongue displayed a modified morphology, with rounded cells detaching from the plaque after being exposed to UVB. Additionally, a significant decrease in the number of cells was observed (Figure 2B).

As for UVB effects on the morphology of HGF cells, the cells showed a rounding and shrinking of their shapes immediately after exposure. There was also a significant reduction in the confluency and the number of cells attached to the plaque (Figure 2B).

3.2. Fluorescence Immunocytochemistry

The structures of the actin fibers and nuclei were examined to gain a better understanding of the effect of the UVB radiation.

A UVB dose of 2.5 J/cm^2 resulted in changes in the nuclei and actin filaments of the tumor cells (Detroit-562 and SCC4). Accordingly, the Detroit-562 cells underwent a series of morphological alterations at the nuclear level, such as the condensation of the nuclei and the formation of the apoptotic bodies. It was observed that the organization of the actin filaments was affected by the exposure to UVB, with a condensation of the filaments and a reorganization occurring at the edge of the cells (Figure 3A). Similar to the Detroit-562 cells, the SCC4 cells experienced nuclear and actin filament changes. As a result, both chromatin condensations and actin filament re-organizations were observed (Figure 3B).
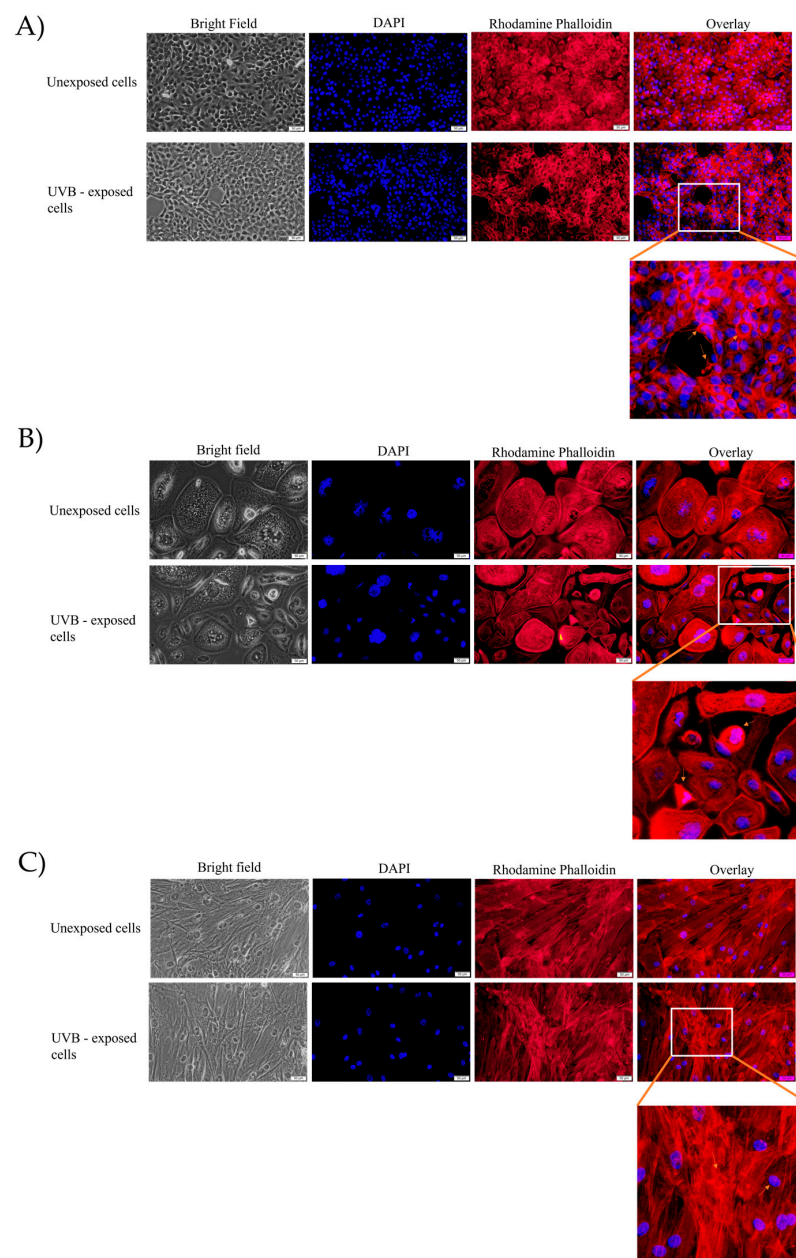

Figure 3. (**A**) Detroit-562 cells, (**B**) SCC4 cells, and (**C**) HGF cells visualized by fluorescence microscopy after exposure to UVB 2.5 J/cm^2. The impact of UVB radiation on the nuclei is shown by DAPI staining (blue) and, for the F-actin fibers, rhodamine phalloidin (red). The yellow arrows highlight the apoptotic-like changes. The scale bar indicates 50 μm.

Although changes were observed at the level of the HGF cells, they were not as severe as those previously observed in the other cell lines. As a result of UVB 2.5 J/cm^2 exposure in this study, the chromatin was slightly condensed, the nuclei were observed to be more compact than the control cells, and the actin filaments were condensed and re-organized with less intensity than those found in the carcinoma cells (Figure 3C). Additionally, the apoptotic index was calculated in order to obtain a more comprehensive view of the nuclear changes (Figure 4).
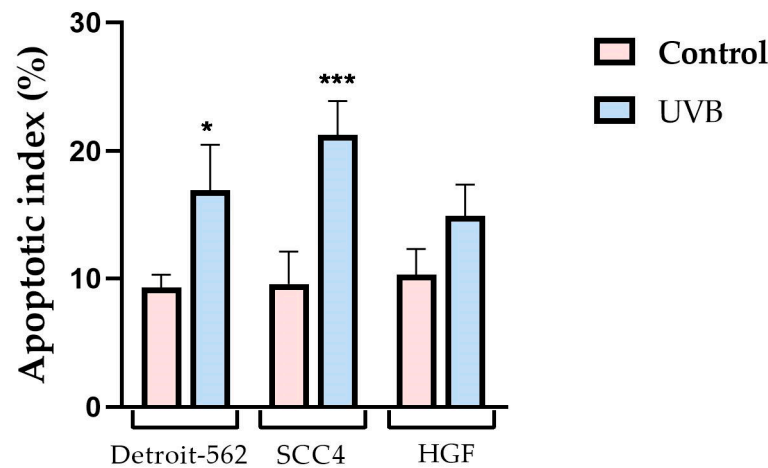

Figure 4. Analysis of the apoptotic index (AI) of Detroit-562, SCC4, and HGF, following exposure to UVB 2.5 J/cm^2. Data are presented as an apoptotic index (%) normalized to control and expressed as mean values ± SD for the three independent experiments. The statistical differences between the control and UVB-exposed cells were verified by applying one-way ANOVA analysis, followed by Dunnett's multiple comparison post hoc test (* $p < 0.05$; *** $p < 0.001$).

Upon exposure to UVB 5 J/cm^2, the Detroit-562 cells showed a series of structural changes on the nuclei and the actin filaments. It was observed that, when exposed to UVB, a strong condensation in the nuclei occurred, as well as fragmentation. A significant amount of condensation was observed in the actin fibers, as well. All these changes suggested an apoptotic-like effect (Figure 5A). In the SCC4 cells, similar changes were observed. It was apparent, therefore, that chromatin was highly condensed in the nuclei. Additionally, condensation was visible in the actin fibers (Figure 5B).
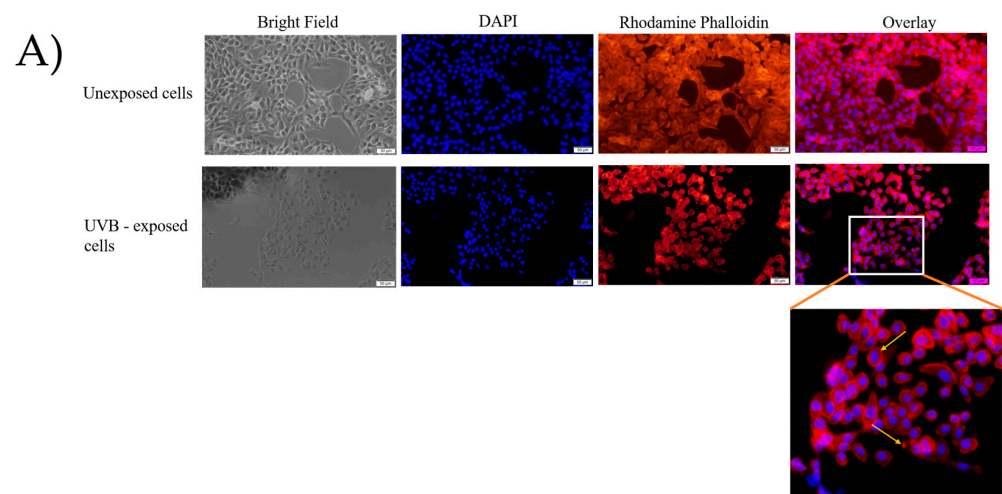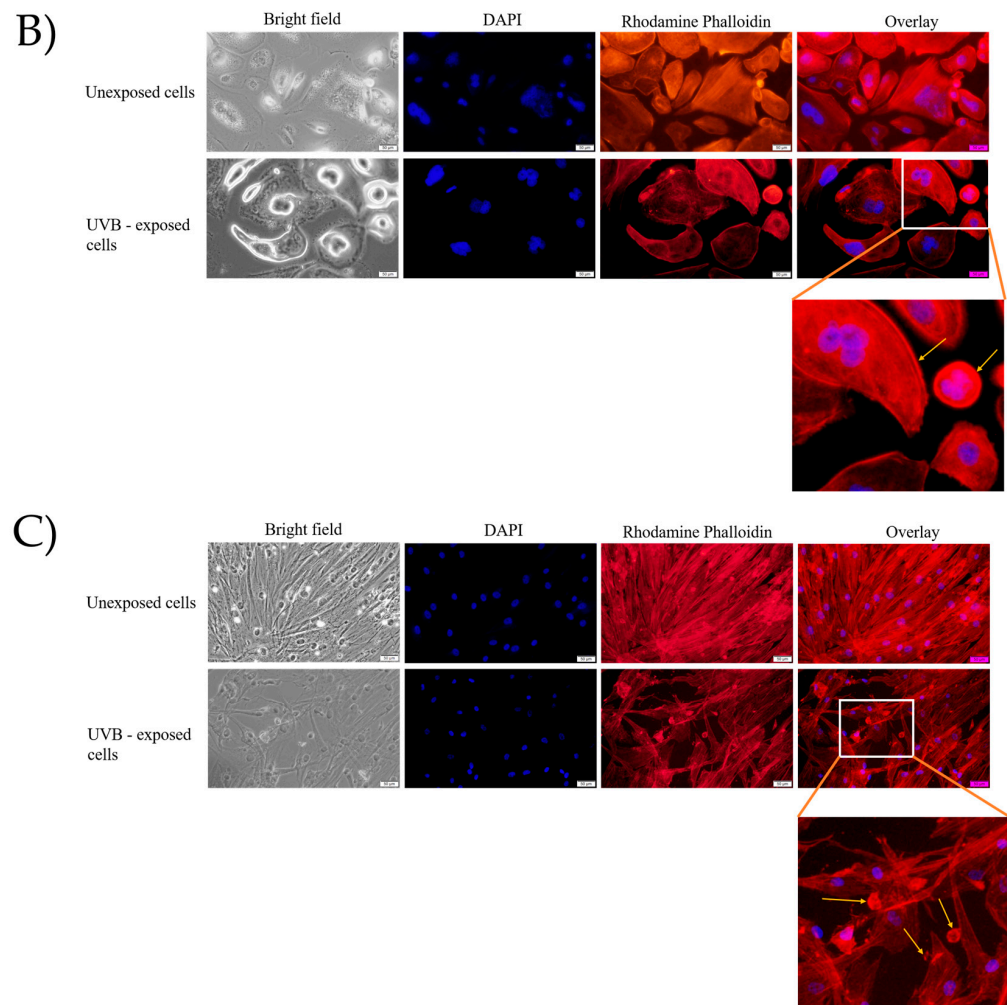

Figure 5. *Cont.*

Figure 5. (**A**) Detroit-562 cells, (**B**) SCC4 cells, and (**C**) HGF cells visualized by fluorescence microscopy, after exposure to UVB 5 J/cm^2. The impact of UVB radiation on the nuclei is shown by DAPI staining (blue) and, for the F-actin fibers, rhodamine phalloidin (red). The yellow arrows highlight the apoptotic-like changes. The scale bar indicates 50 μm.

The HGF cells were adversely affected by UVB in terms of their nuclei and actin filament structures. At the level of the nucleus, chromatin condensation was observed immediately following exposure. Additionally, a ring-shaped condensation in the actin filaments was found at the periphery of the cells. These changes were characteristic of the apoptosis process and were consistent with the results of the previous test for cell viability (Figure 5C). Using the apoptotic index (AI), it was determined that UVB exerted a significant pro-apoptotic effect on all the analyzed cells (Figure 6).

In addition, by evaluating the area and the circumference of the cellular nuclei exposed to UVB 2.5 J/cm^2, it was found that in all the exposed cells, there was a decrease in the area of the nuclei, with tumor cells exhibiting the greatest area reduction (Figure 7A–C). The circumference, on the other hand, did not show significant changes, as compared to the control cells (Figure 7D).
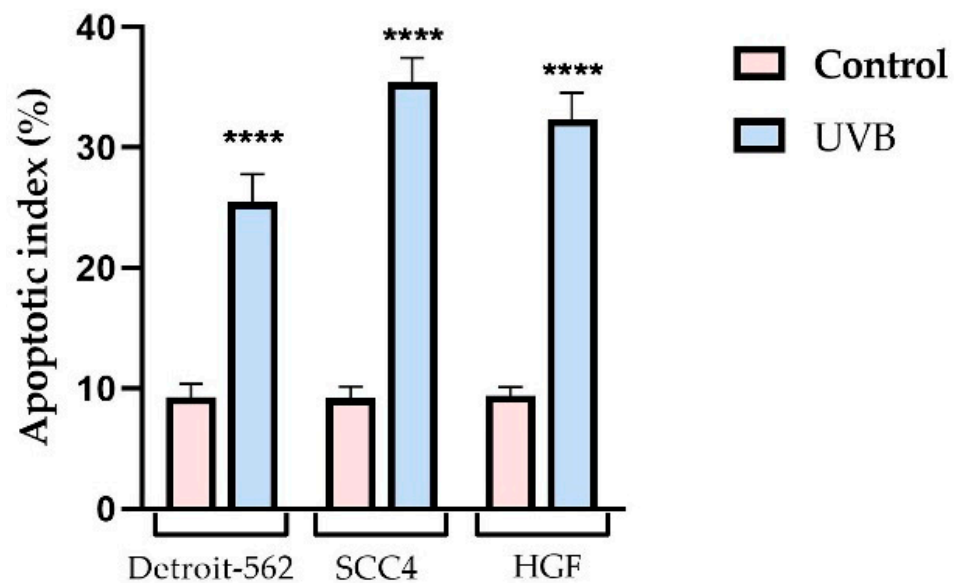
Figure 6. Analysis of the apoptotic index (AI) of Detroit-562, SCC4, and HGF, following exposure to UVB 5 J/cm^2. Data are presented as an apoptotic index (%) normalized to control and expressed as mean values $\pm$ SD for the three independent experiments. The statistical differences between the control and exposure cells were verified by applying a one-way ANOVA analysis, followed by Dunnett's multiple comparison post hoc test (**** $p < 0.0001$).
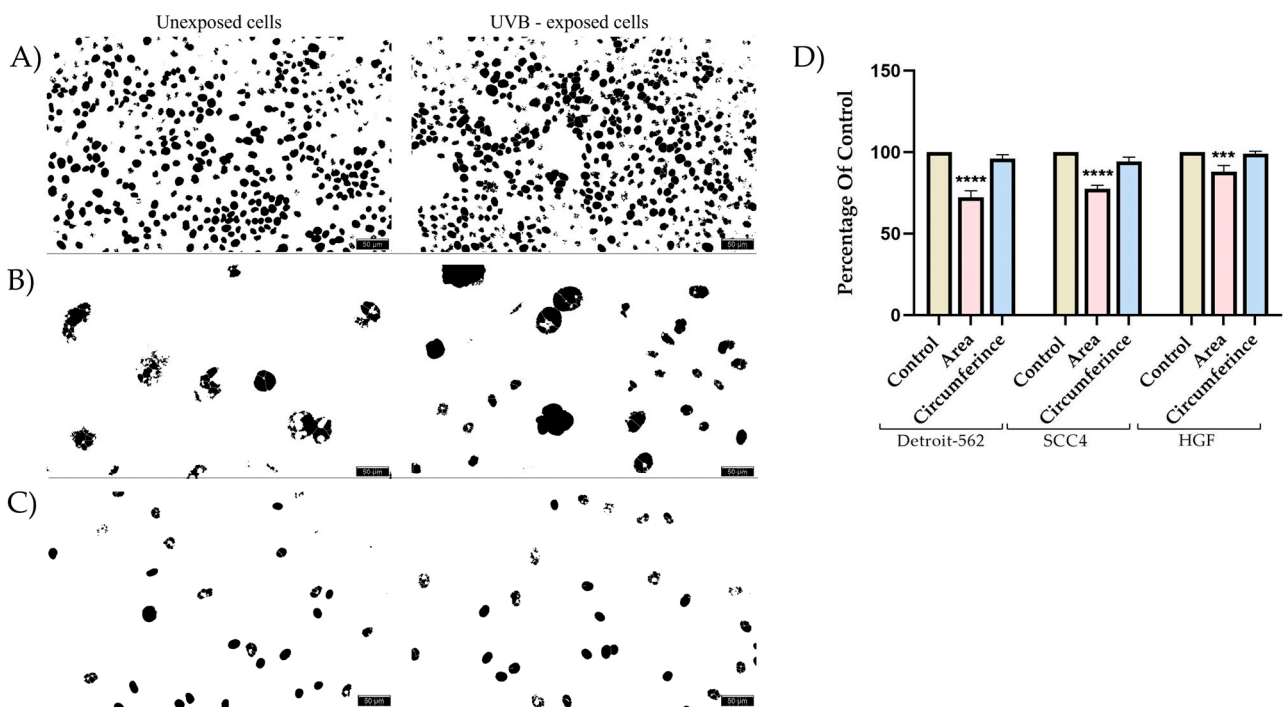

Figure 7. Evaluation of cell nuclei of (**A**) Detroit-562, (**B**) SCC4, and (**C**) HGF cells, after conversion to 8-bit images and application of the make-binary function. (**D**) As compared to the control cells, the cells exposed to UVB (2.5 J/cm^2) showed a decrease in their nuclear area as well as their nuclear circumferences. The statistical differences between control and exposed cells were verified by applying one-way ANOVA analysis, followed by Dunnett's multiple comparison post hoc test (*** $p < 0.001$; **** $p < 0.0001$).

Moreover, as compared to the control cells, the cells exposed to UVB 5 J/cm^2 showed a decrease in their nuclear area (Figure 8A–C). In terms of the circumference of the nu-

cleus after exposure to UVB, there was no statistically significant decrease recorded; the difference between the circumference of the control cells and the cells exposed to UVB was approximately 2–3% (Figure 8D).
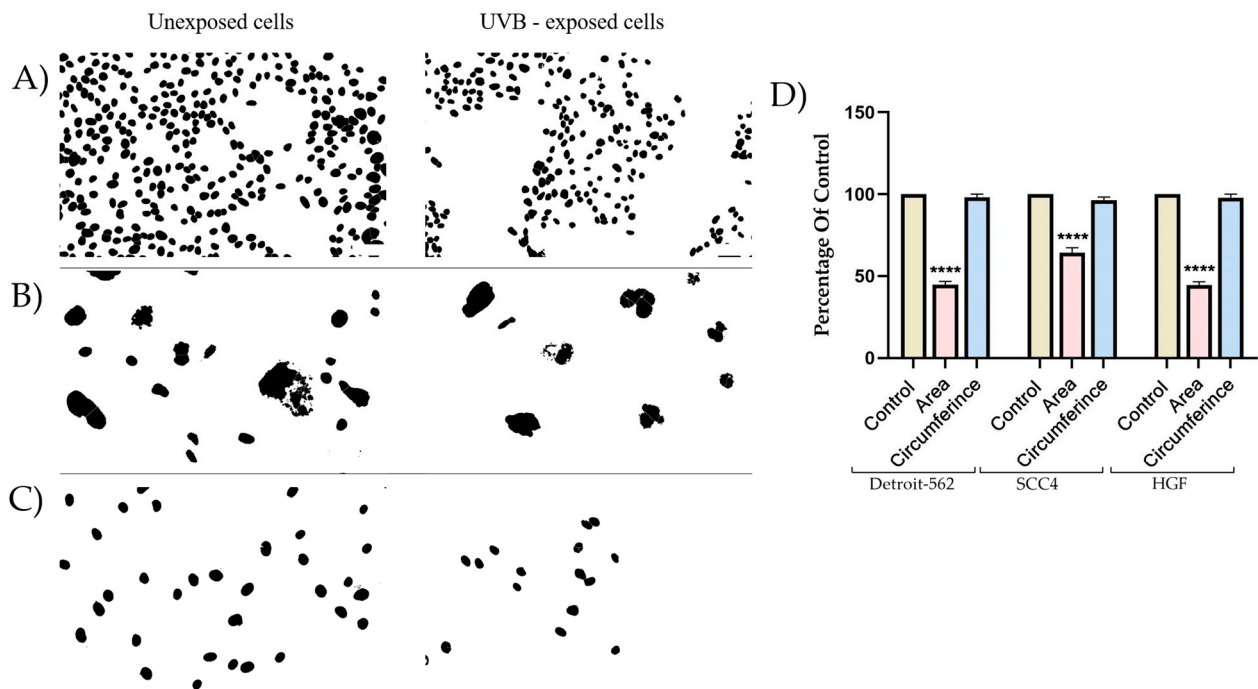

Figure 8. Evaluation of cell nuclei of the (**A**) Detroit-562, (**B**) SCC4, and (**C**) HGF cells, after conversion to 8-bit images and the application of the make-binary function. (**D**) As compared to the control cells, the cells exposed to UVB ($5\,J/cm^2$) showed a decrease in their nuclear area as well as their nuclear circumference. The statistical differences between control and exposure cells were verified by applying a one-way ANOVA analysis, followed by Dunnett's multiple comparison post hoc test (**** $p < 0.0001$).

3.3. Gene Expression Ratio

According to the previous results obtained in the cell viability test, the exposure to UVB caused a decrease in cell viability. After the immunofluorescence analysis at the nucleus and actin filament level, the changes observed in the Detroit-562, SCC4, and HGF cells that were characteristic of the apoptosis process. Therefore, the next step was to assess the expression of the genes involved in apoptosis, namely Bcl-2, an anti-apoptotic gene, and Bax, a pro-apoptotic gene.

UVB exposure, at a dose of $2.5\,J/cm^2$, decreased the expression of the anti-apoptotic gene (Bcl-2) in all the analyzed cells, but the decrease was not statistically significant. Moreover, in the tumor cells, a significant increase in the expression of the pro-apoptotic gene (Bax) was found. In contrast, the HGF cells did not exhibit a significant increase in Bax gene expression (Figure 9).

The graphic in Figure 10 shows that, after UVB $5\,J/cm^2$ exposure, both tumor cells (Detroit-562 and SCC4) and healthy gingival fibroblast cells (HGF) showed a decrease in the expression of the anti-apoptotic gene (Bcl-2), while the pro-apoptotic gene (Bax) increased. It was important to note that the increase in the Bax gene expression was similar in both the tumor and healthy cells, with no statistically significant differences.
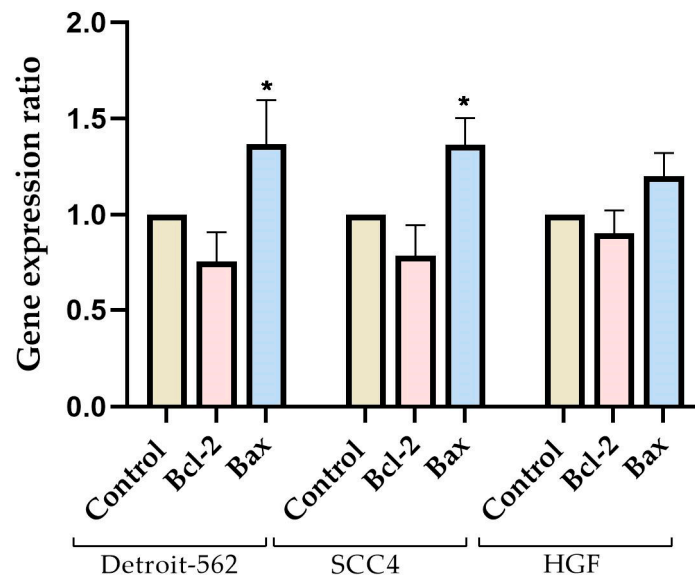
Figure 9. Relative fold-change expression of mRNA of pro-apoptotic (Bax) and anti-apoptotic (Bcl-2) markers in Detroit-562, SCC4, and HGF cells immediately after UVB (2.5 J/cm^2) exposure. The mRNA expression levels were normalized to 18 S expression, and the mean values $\pm$ SD of the three independent experiments were presented based on a one-way ANOVA analysis with Dunnett's post hoc test, which were used to identify the statistical differences (* $p < 0.05$).
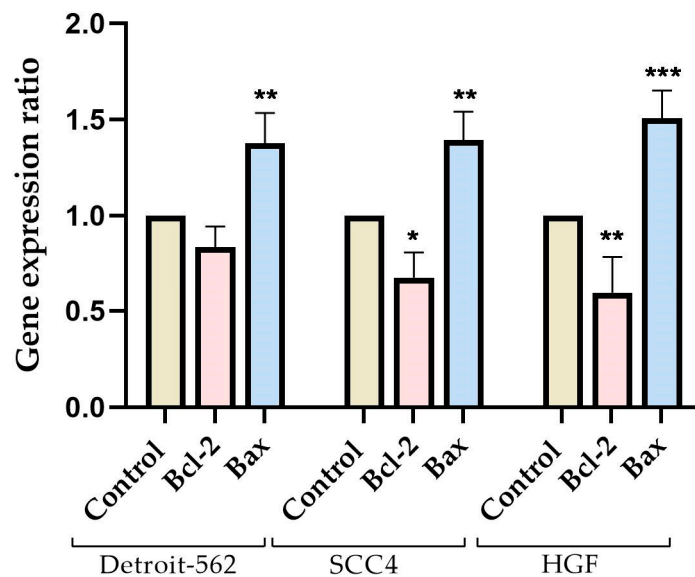

Figure 10. Relative fold-change expression of mRNA of pro-apoptotic (Bax) and anti-apoptotic (Bcl-2) markers in Detroit-562, SCC4, and HGF cells immediately after UVB (5 J/cm^2) exposure. The mRNA expression levels were normalized to 18 S expression, and the mean values $\pm$ SD of the three independent experiments were presented based on a one-way ANOVA analysis with Dunnett's post hoc test, which were used to identify the statistical differences (* $p < 0.05$; ** $p < 0.01$ and *** $p < 0.001$).

3.4. Caspase Activity

After exposure to UVB, the Detroit-562, SCC4, and HGF cells were tested for apoptosis using Caspase-Glo 3/7, 8, and 9 kits. These kits monitored the activity of caspases-3/7, 8, and 9 in the cells.

In response to UVB exposure at an intensity of 2.5 J/cm^2, the caspase activity changed. Accordingly, all analyzed caspases displayed a similar increase in activity in the tumor cells, with caspase-3/7 exhibiting the highest level of activity. A significant increase in

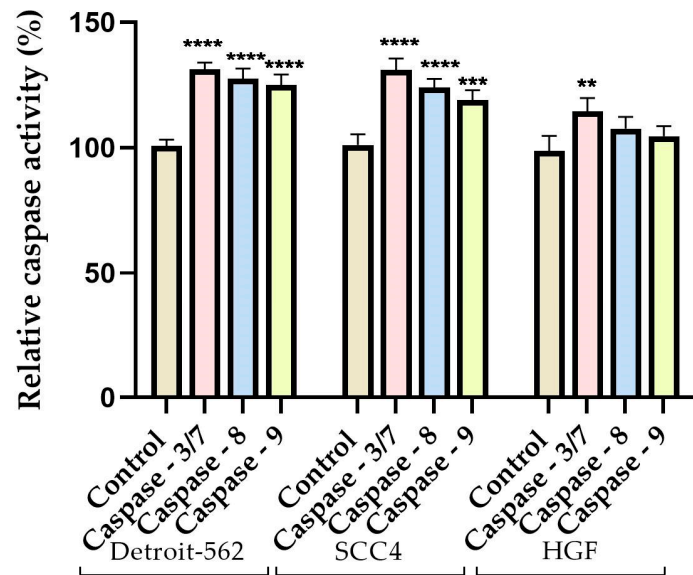caspase-3/7 was observed in healthy cells, while caspases-8 and -9 showed no significant increase (Figure 11).

Figure 11. Induction of caspases-3/7, 8, and 9 in Detroit-562, SCC4, and HGF cells, after UVB (2.5 J/cm^2) exposure. Data are presented as mean ± SD of the three independent experiments, in reference to the non-exposure group. One-way ANOVA and Dunnett's post hoc test were used to identify the statistical differences (** $p < 0.01$; *** $p < 0.001$ and **** $p < 0.0001$).

The tumor cells exhibited increased luminescence after UVB exposure at a dose of 5 J/cm^2, which indicated a significant increase in the activity of caspase-3/7. Furthermore, an important increase was also observed in the activity of caspases-8 and 9. In the gingival fibroblasts, similar changes were observed, with all the analyzed caspases showing increased activity. According to a statistical analysis, caspases-3/7 and 8 exhibited the greatest increase in activity (Figure 12).
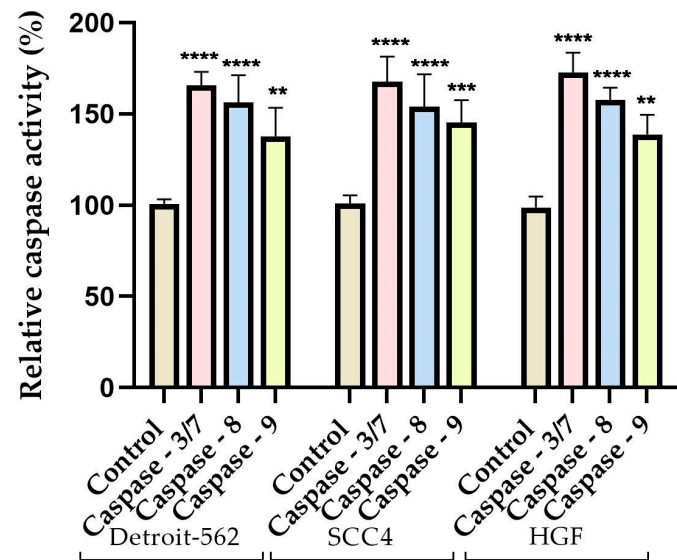

Figure 12. Induction of caspases-3/7, 8, and 9 in Detroit-562, SCC4, and HGF cells, after UVB (5 J/cm^2) exposure. Data are presented as mean ± SD of three independent experiments, in reference to the non-exposure group. One-way ANOVA and Dunnett's post hoc test were used to identify the statistical differences (** $p < 0.01$; *** $p < 0.001$ and **** $p < 0.0001$).

4. Discussion

Numerous studies on ultraviolet radiation have revealed its negative effects on human health, particularly as it pertains to tumor development [31–33]. However, UVR is also used for medical purposes, such as the treatment of psoriasis and cutaneous T-cell lymphoma via phototherapy [34]. As another contribution of UV radiation, UVR is capable of initiating a chemical reaction that resulted in pre-vitamin D3 being produced by 7-dehydrocholesterol [35]. Furthermore, UVR has also been found to be useful in the field of dental medicine, both for diagnostic and therapeutic purposes [36]. According to a study conducted in the United States, ultraviolet radiation has the potential to increase the risk of cancer in not only the skin but in other tissues, as well, and has been associated with oral, pharyngeal, and cervical cancers, among others [2]. Although the World Health Organization has recognized UVR as a strong human carcinogen, there has not been a safe limit determined for the exposure of internal tissues to UVR [37]. Therefore, the present study evaluated the impact of UVB exposure at two doses (2.5 and 5 J/cm^2) on two types of oral carcinoma calls (tongue and pharyngeal), as well as on healthy gingival fibroblasts. The present study aimed to evaluate the behavior of cells at elevated doses of UVB, as the data regarding dental cells exposed to ultraviolet radiation were scarce and incomplete.

Previous studies examined UVB's effects on a variety of cell lines, including myeloid leukemia, T-lymphoblastoid Molt-4, skin-derived primary fibroblasts, keratinocytes, and human tissues reconstructed from skin, gingiva, and oral tissues [37–40]. Moreover, UVB has been commonly used for diagnostic and treatment purposes in dental practices at a maximum intensity of 5 J/cm^2 [36]. Therefore, in this study, the doses of the UVB exposure on the selected cell lines were based on the evidence presented in the literature. Khalil assessed the effect of UVB on human skin fibroblasts using UVB doses of up to 5.6 J/cm^2 [41]. Additionally, Khalil and Shebaby evaluated the cytotoxicity of UVB on human-derived skin cells using UVB doses between 0 and 5.6 J/cm^2 [42]. There have been relatively few studies that evaluated the UVB effect on oral fibroblasts and other types of cells in the oral cavity. In one of the few studies, Boza and colleagues examined the effects of UVB radiation on oral mucosal fibroblasts and found that UV radiation caused a marked decrease in cell proliferation [43]. In addition, studies have investigated the effect of UVB radiation on lung mucosa fibroblasts and skin fibroblasts. For example, Straface and their research group exposed lung mucosal fibroblasts to a subtoxic dose of UVB at 200 mJ/cm^2 and found that cell proliferation decreased [44]. A similar decrease in cell viability and proliferation was observed in a study by Chainiaux et al., who exposed human skin fibroblasts to repeated doses of UVB at 62.5 mJ/cm^2 [45]. A dose of 3.25 J/cm^2 of UVB exhibited similar effects on human dermal fibroblasts, including a decrease in proliferation and signs of autophagy and apoptosis [46]. There was a strong correlation between the results of these studies and the results obtained in the present study, regarding UVB's effect on gingival fibroblasts. The present study highlighted a cytotoxic and pro-apoptotic effect of UVB on Detroit-562 and SCC4 cells, immediately following exposure. Kimura and colleagues also exposed various types of cells to UVB, including human osteosarcoma cells, human fibrosarcoma cells, Lewis lung carcinoma, and XPA-1 human pancreatic cancer cells, and they determined that UVB had a cytotoxic effect, with cell death being observed even after 10 h of exposure to UVB [47]. According to a study conducted on cervical cancer cells, UVB exposure had a pronounced cytotoxic and pro-apoptotic effect, leading to a marked decline in cell viability [48]. Furthermore, Wang and colleagues evaluated the effect of UVB on breast cancer cells, concluding that UVB combined with coenzyme Q$_0$ produces an intense cytotoxic response [49]. Moreover, Sarkar et al. speculated that UVB might be used in antitumor therapy in breast cancer after finding that UVB decreased tumor cell viability selectively without affecting healthy cells [50]. Although UVB radiation as a risk factor for the development of oral cancers has been highlighted, to the best of our knowledge, the in vitro effect on pharynx and tongue cancer cells had not yet been evaluated.

In the present study, two oral carcinoma cell lines (pharyngeal and tongue) and a healthy gingival fibroblast cell line were selected for the evaluation of the effect of UVB

exposure. As a result of the assessment of cell viability, it was found that the exposure to UVB decreased the viability in both pharyngeal and tongue carcinoma cells, as well as in healthy gingival fibroblasts, where the strongest cytotoxic effect was observed. The most significant decrease in cell viability was observed after the cells had been exposed to UVB at a dose of 5 J/cm2. Therefore, at 2.5 J/cm^2, the viability of the Detroit-562 and SCC4 cells decreased to approximately 66% and 65%, respectively. In contrast, the gingival fibroblasts were not as strongly affected, with a viability of approximately 81%. On the other hand, in tumor cells, the viability of the cells obtained immediately following exposure to UVB 5 J/cm^2 was approximately 66% in the Detroit-562 cells and approximately 56% in the SCC4 cells. Immediately following UVB exposure, the HGF cell viability decreased to approximately 45%. UVB intensities of 2.5 and 5 J/cm^2 were used on the cells. Having observed the cytotoxic effects of UVB on Detroit-562, SCC4, and HGF cells, the next step was to determine the effect of UVB on the cellular morphology, nuclei, and actin filament structures. Upon exposure to 2.5 J/cm^2 of UVB, changes in the morphological, nuclear, and actin filament structures were observed, especially in tumor cells. There was evidence of chromatin condensation, and the actin filaments formed a peripheral ring-like arrangement. Regarding the impact of UVB on the tumor cells, it was noted that the exposure to UVB at 5 J/cm^2 resulted in a marked decrease in the number of cells, as well as shape changes, with the cells becoming rounded and detaching from the plate. It was also observed that the healthy gingival fibroblast cells underwent important morphological changes following exposure to UVB, including rounding, detachment from plaque, shrinkage, and a reduction in cell number. Additionally, a dose of 5 J/cm^2 induced strong condensation on the tumor cell nuclei and actin filaments, which were condensed in the form of a ring around the periphery. A similar pattern of changes was observed in the HGF cells, with the nuclei and actin filaments showing areas of condensation. The changing morphological characteristics were used to identify the type of cell death that was responsible for the decrease in cell viability. Therefore, during apoptosis, the cells underwent the stereotypical changes that primarily occurred within the nucleus and cytoplasm [51]. Apoptosis is characterized by cell contraction and is one of the most well-known characteristics of the process [52]. A further consequence of the decreasing size of the cells was the loss of contact with the neighboring cells, as well as the detachment from the extracellular matrix. After detachment, the focal adhesions underwent re-organization, resulting in the morphological changes, such as rounded cell shapes. Afterwards, the membrane blebbing occurred, which required the re-organization of the actin cytoskeleton as well as the activation of the myosin chains through phosphorylation. Finally, the strong condensation of the cells led to the formation of the apoptotic bodies [53]. Fluorescent microscopy is a popular technique for studying the apoptosis process, as DAPI (4,6-diamidino-2-phenylindole-dihydrochloride) binds to cell nuclei with a strong affinity. This method has demonstrated a selectivity for DNA, having been successfully used to identify the condensed chromatin in apoptotic nuclei [54]. Visually, apoptotic nuclei may appear to be smaller than normal nuclei, and condensed chromatin appears bright fluorescent. A further advantage of this technique is the ability to visualize nuclear fragments, which is another characteristic of apoptosis [55]. Because of these changes in the nuclear structure, the particularities of the process of apoptosis, including the morphological characteristics such as nuclear area and circumference, have been used to indicate the activation of programmed cell death [30]. An analysis of the nuclear area and circumference of the nuclei was performed using the ImageJ program. As a result of their exposure to UVB at a dose of 2.5 J/cm^2, all the analyzed cells exhibited a significant decrease in their nuclei area. However, there were no significant changes in the circumferences of the nuclei. Meanwhile, the exposure to UVB at a dose of 5 J/cm^2 was associated with an even more pronounced decrease in the nuclear area, which was accompanied by a slight reduction in the nuclear circumference. In order to distinguish between apoptotic and necrotic cell deaths, it was important to observe these changes at the nuclear level. In apoptosis, the nucleus would undergo early morphological changes, and in necrosis, the nucleus would remain relatively unaltered

while the membranes and organelles would show early signs of alteration [56]. In apoptosis, caspases initiated the destruction of the nuclear envelope, which then led to morphological changes. Furthermore, during the early stages of programmed cell death, nuclei underwent changes in a caspase-independent manner, through Bax, and this led to the rupture of the nuclear bubbles and the release of the apoptogenic nuclear proteins into the cytosol, thereby promoting cell death. Therefore, the nuclear envelope could play a key role in the early stages of apoptosis [57]. In addition, a large number of proteins are involved in the process of apoptosis, the most prominent of which is actin. The actin protein participates in the regulation and maintenance of the shape of cells by forming microfilaments [58]. An apoptotic cell undergoes a re-organization of its cytoskeleton and a fragmentation of its microfilament bundles, resulting in a decrease in volume and the contraction of the cell. Consequently, actin microfilaments undergo re-organization, forming bundles that are progressively more condensed and thicker, and which are located near the periphery of the cell [51]. It was easiest to observe this rearrangement of the cytoskeleton by staining for actin. Because actin is the most abundant component of the cytoskeleton, its re-organization and splitting are distinctive characteristics of the delayed stage of apoptosis [59]. All of these morphological changes in the cells were observed in this study after cell exposure to UVB, suggesting that UVB had an apoptotic-like effect.

An investigation of the expression of the anti-apoptotic (Bcl-2) and pro-apoptotic (Bax) genes was conducted to determine the type of cell death induced by UVB exposure more precisely. A dose of 2.5 J/cm^2 increased the expression of the pro-apoptotic marker Bax, especially in tumor cells, while the expression of the Bcl-2 gene was relatively low, as compared to the control cells, but not significantly different. Furthermore, UVB (5 J/cm^2) decreased the expression of the Bcl-2 gene, whereas the pro-apoptotic gene, Bax, increased in expression in all types of cells exposed to UVB. Based on these results, UVB exposure could induce cytotoxicity through the stimulation of apoptosis. As part of the p53 Bax–Bak pathway, Bcl-2 plays an important role [60]. It has been demonstrated in a similar study that UVB induced the death of keratinocytes by reducing the expression of the Bcl-2 gene [61]. A study conducted by Trabosh and colleagues demonstrated that UVB exposure increased Bax expression in human keratinocytes [62]. Moreover, melanocytes exposed to UVB exhibited an upregulation of the Bax gene [63]. Furthermore, the impact of UVB on the human epidermoid carcinoma cell line was studied, and the researchers demonstrated that low doses of UVB led to a decrease in the expression of Bcl-2, whereas doses exceeding 35 mJ/cm^2 delayed the decrease in Bcl-2 expression, which, in turn, delayed apoptosis [64]. Furthermore, the UV treatment of lung adenocarcinoma cells induced apoptosis that was dependent on the Bax gene expression increase [65]. The Bcl-2 family of proteins is known to play an important role in regulating apoptosis. Although the mechanism by which Bcl-2 proteins are involved in programmed cell death remains unclear, though one aspect is certain: they modulate the release of proteins from the intermembrane space of the mitochondria. Bcl-2 is a family of proteins that includes both the pro-apoptotic (Bax) and anti-apoptotic (Bcl-2) proteins [66]. An important feature of Bax is that it contains 4 BH (Bcl-2 homology) domains and is one of the key regulators of apoptosis, acting downstream of anti-apoptotic proteins [67]. Moreover, by decreasing Bcl-2 expression, the anti-apoptotic properties of Bcl-2 were inhibited while Bax oligomerization was induced, which promoted apoptosis [68].

In addition to these changes, another feature of the apoptosis process is the activation of an intracellular cysteine endopeptidase family, known as caspases. Caspases-8 and 9 play the role of initiating gatekeepers, whereas caspase-3 and 7 play the role of executors. In the activation of caspases, Bax is known to play an important role in the release of cytochrome c from the mitochondrial intermembrane space into the cytoplasm, which ultimately results in the formation of a multi-metric complex known as an "apoptosome". Apoptosomes function as activators of caspase-9, which, once activated, targets caspase-3, one of the effector caspases [69]. Therefore, external factors that activate initiating caspases are likely to activate caspase-3, resulting in a series of events that translate into

cell lysis and the disruption of normal cellular functions [70]. As a key player in mediating nuclear apoptosis, caspase-3 contributes to the condensing of the nuclear structure, the fragmentation of DNA, and the blebbing of cellular membranes [71]. Since many caspases can cleave the same substrate in vitro, caspase-3 and caspase-7 share the same recognition sequence [72]. Therefore, the present study evaluated the activity of both types of caspases. The process of apoptosis was primarily mediated through the intrinsic (mitochondrial) or extrinsic (mediated by death receptors) pathways. Among the caspases, caspase-9 initiated the extrinsic apoptotic pathway, while caspase-8 initiated the intrinsic apoptotic pathway [73]. UVB has been shown to induce apoptosis at the cellular level through the activation of both intrinsic and extrinsic pathways in previous studies [74,75]. According to a study by Park and Jang, the exposure to UVB increased caspase-9 expression in human keratinocytes [76]. Similarly, Xu and colleagues observed that the exposure to UVB activated caspase-8 and caspase-3 in human skin fibroblasts [77]. Takasawa et al. found that UVB exposure caused caspase-8 activation in human keratinocytes, whereas UVC did not. Furthermore, researchers have demonstrated that UVB was dependent on caspase-8 to induce apoptosis through both intrinsic and extrinsic pathways, whereas UVC induced apoptosis only through intrinsic pathways [78]. These results were in agreement with those obtained in the current study. Furthermore, UVB (2.5 J/cm^2) significantly increased the activity of caspases-3/7, 8, and 9 in tumor cells, whereas only caspase-3/7 activity was significantly increased in healthy cells. Comparatively, UVB (5 J/cm^2) exposure determined the increase in caspases-8, 9 and 3/7 activity in all 3 cell lines studied, among which, caspase-3/7 presented the highest activity. Caspase-3 is responsible for initiating the characteristic signs of apoptosis, which include contractions and the blebbing of the membrane of the cell [79]. Accordingly, the increase in activity observed in the current study was consistent with the changes observed on a morphological level. According to the present study, decreasing the Bcl-2 expression resulted in the loss of Bcl-2's inhibitory effect on Bax and the caspase cascade, which, in turn, caused the overexpression of Bax and the activation of caspases 9 and 3/7, which was characteristic of an extrinsic apoptosis process. Moreover, caspase-8, which is associated with intrinsically mediated cell death, was observed to increase in expression.

5. Conclusions

It was concluded that UVB (5 J/cm^2) had a cytotoxic effect on both tumor cells (Detroit-562 and SCC4) and gingival fibroblasts (HGF), which resulted in a series of changes: (i) a significant reduction in cell viability, especially in HGF cells, where the viability dropped below 50%; (ii) decreased cell confluency and adhesion, along with altered morphology; (iii) the induction of apoptotic changes (cell rounding, the condensation of the nuclei, the re-organization of the actin filaments); and (iv) an increase in the expression of the pro-apoptotic gene (Bax), followed by the decrease in the expression of the anti-apoptotic gene (Bcl-2), indicating that UVB had induced apoptosis in both tumor and healthy cells. The apoptotic changes that were characteristic of both intrinsic and extrinsic pathways were induced by UVB exposure, as corroborated by the expression patterns of the caspases that played a critical role in these processes. These changes (decreases in cell viability, the induction of morphological changes, the appearance of alterations in the structures of the nuclei and actin filaments, the increase in the expression of the pro-apoptotic markers, and the decrease in anti-apoptotic markers, together with the increase in the activity of caspases-3/7, 8, and 9) suggested an apoptotic-like effect that was primarily observed in the tumor cells, whereas the healthy oral cells were not significantly affected when exposed to UVB at a dose of 2.5 J/cm^2. Therefore, it is important to recognize the difference between the effects of UVB on healthy and tumor cells, based on the dose of applied UVB. There is, however, a need for additional studies to understand the biological mechanisms underlying UVB's effects and to determine if these changes persist over time, as well as to affirm the maximum dose to which these types of cells should be exposed.

References

1. Moan, J.; Grigalavicius, M.; Baturaite, Z.; Dahlback, A.; Juzeniene, A. The Relationship between UV Exposure and Incidence of Skin Cancer. *Photodermatol. Photoimmunol. Photomed.* **2015**, *31*, 26–35. [CrossRef]
2. Adams, S.; Lin, J.I.E.; Brown, D.; Shriver, C.D.; Zhu, K. Ultraviolet Radiation Exposure and the Incidence of Oral, Pharyngeal and Cervical Cancer and Melanoma: An Analysis of the SEER Data. *Anticancer. Res.* **2016**, *36*, 233–237.
3. Dale Wilson, B.; Moon, S.; Armstrong, F. Comprehensive Review of Ultraviolet Radiation and the Current Status on Sunscreens. *J. Clin. Aesthetic Dermatol.* **2012**, *5*, 18.
4. Kumar, R.; Deep, G.; Agarwal, R. An Overview of Ultraviolet B Radiation-Induced Skin Cancer Chemoprevention by Silibinin. *Curr. Pharmacol. Rep.* **2015**, *1*, 206–215. [CrossRef]
5. El Ghissassi, F.; Baan, R.; Straif, K.; Grosse, Y.; Secretan, B.; Bouvard, V.; Benbrahim-Tallaa, L.; Guha, N.; Freeman, C.; Galichet, L.; et al. A Review of Human Carcinogens—Part D: Radiation. *Lancet Oncol.* **2009**, *10*, 751–752. [CrossRef]
6. Katiyar, S.K.; Singh, T.; Prasad, R.; Sun, Q.; Vaid, M. Epigenetic Alterations in Ultraviolet Radiation-Induced Skin Carcinogenesis: Interaction of Bioactive Dietary Components on Epigenetic Targets. *Photochem. Photobiol.* **2012**, *88*, 1066–1074. [CrossRef]
7. de Oliveira, N.F.; de Souza, B.F.; de Castro Coêlho, M. UV Radiation and Its Relation to DNA Methylation in Epidermal Cells: A Review. *Epigenomes* **2020**, *4*, 23. [CrossRef]
8. Gentile, M.; Latonen, L.; Laiho, M. Cell Cycle Arrest and Apoptosis Provoked by UV Radiation-induced DNA Damage Are Transcriptionally Highly Divergent Responses. *Nucleic Acids Res.* **2003**, *31*, 4779–4790. [CrossRef]
9. Cha Jun, H.; Kim, O.; Lee Tai, G.; Lee Sik, K.; Lee Ho, J.; Park, I.; Lee, S.; Kim Ri, Y.; Ahn Joong, K.; An, I.; et al. Identification of Ultraviolet B Radiation-induced MicroRNAs in Normal Human Dermal Papilla Cells. *Mol. Med. Rep.* **2014**, *10*, 1663–1670. [CrossRef]
10. Watson, M.; Holman, D.M.; Maguire-Eisen, M. Ultraviolet Radiation Exposure and Its Impact on Skin Cancer Risk. *Semin. Oncol. Nurs.* **2016**, *32*, 241–254. [CrossRef]
11. Bush, M.A.; Hermanson, A.S.; Yetto, R.J.; Wieczkowski, G.J. The Use of Ultraviolet LED Illumination for Composite Resin Removal: An In Vitro Study. *Gen. Dent.* **2010**, *58*, e214–e218.
12. McGee, S.; Mirkovic, J.; Mardirossian, V.; Elackattu, A.; Yu, C.-C.; Kabani, S.; Gallagher, G.; Pistey, R.; Galindo, L.; Badizadegan, K.; et al. Model-Based Spectroscopic Analysis of the Oral Cavity: Impact of Anatomy. *J. Biomed. Opt.* **2008**, *13*, 64034. [CrossRef]
13. McGee, S.; Mardirossian, V.; Elackattu, A.; Mirkovic, J.; Pistey, R.; Gallagher, G.; Kabani, S.; Yu, C.-C.; Wang, Z.; Badizadegan, K.; et al. Anatomy-Based Algorithms for Detecting Oral Cancer Using Reflectance and Fluorescence Spectroscopy. *Ann. Otol. Rhinol. Laryngol.* **2009**, *118*, 817–826. [CrossRef]
14. Duarte, I.A.G.; Hafner, M.D.F.S.; Malvestiti, A.A. Ultraviolet Radiation Emitted by Lamps, TVs, Tablets and Computers: Are There Risks for the Population? *An. Bras. Dermatol.* **2015**, *90*, 595–597. [CrossRef]
15. Morais, P. Artificial Tanning Devices (Sunbeds): Where Do We Stand? *Cutan. Ocul. Toxicol.* **2022**, *41*, 123–128. [CrossRef]
16. Bruzell, E.M.; Johnsen, B.; Aalerud, T.N.; Dahl, J.E.; Christensen, T. In Vitro Efficacy and Risk for Adverse Effects of Light-Assisted Tooth Bleaching. *Photochem. Photobiol. Sci.* **2009**, *8*, 377–385. [CrossRef]
17. Rudhart, S.A.; Günther, F.; Dapper, L.; Thangavelu, K.; Gehrt, F.; Stankovic, P.; Wilhelm, T.; Guenzel, T.; Stuck, B.A.; Hoch, S. UV Light-Based Decontamination: An Effective and Fast Way for Disinfection of Endoscopes in Otorhinolaryngology? *Eur. Arch. Oto-Rhino-Laryngol.* **2020**, *277*, 2363–2369. [CrossRef]
18. Liu, K.; Shang, C.; Wang, Z.; Qi, Y.; Miao, R.; Liu, K.; Liu, T.; Fang, Y. Non-Contact Identification and Differentiation of Illicit Drugs Using Fluorescent Films. *Nat. Commun.* **2018**, *9*, 1695. [CrossRef]
19. Herrington, W.F.; Singh, G.P.; Wu, D.; Barone, P.W.; Hancock, W.; Ram, R.J. Optical Detection of Degraded Therapeutic Proteins. *Sci. Rep.* **2018**, *8*, 5089. [CrossRef]
20. Mojeski, J.A.; Almashali, M.; Jowdy, P.; Fitzgerald, M.E.; Brady, K.L.; Zeitouni, N.C.; Colegio, O.R.; Paragh, G. Ultraviolet Imaging in Dermatology. *Photodiagnosis Photodyn. Ther.* **2020**, *30*, 101743. [CrossRef]

21. Xu, Q.; McMichael, P.; Creagh-Flynn, J.; Zhou, D.; Gao, Y.; Li, X.; Wang, X.; Wang, W. Double-Cross-Linked Hydrogel Strengthened by UV Irradiation from a Hyperbranched PEG-Based Trifunctional Polymer. *ACS Macro Lett.* **2018**, *7*, 509–513. [CrossRef]

22. Branisteanu Elena, D.; Dirzu Stefania, D.; Toader Paula, M.; Branisteanu Constantin, D.; Nicolescu Codrut, A.; Brihan, I.; Bogdanici Margareta, C.; Branisteanu, G.; Dimitriu, A.; Anton, N.; et al. Phototherapy in Dermatological Maladies (Review). *Exp. Ther. Med.* **2022**, *23*, 259. [CrossRef]

23. de Oliveira, B.P.; Aguiar, C.M.; Câmara, A.C.; de Albuquerque, M.M.; Correia, A.C.R.D.B.; Soares, M.F.D.L.R. The Efficacy of Photodynamic Therapy and Sodium Hypochlorite in Root Canal Disinfection by a Single-File Instrumentation Technique. *Photodiagnosis Photodyn. Ther.* **2015**, *12*, 436–443. [CrossRef]

24. Haraguchi, A.; Yoshida, S.; Takeshita, M.; Sumi, Y.; Mitarai, H.; Yuda, A.; Wada, H.; Nishimura, F.; Maeda, H.; Wada, N. Effects of Ultraviolet Irradiation Equipment on Endodontic Disease–Related Bacteria. *Lasers Dent. Sci.* **2022**, *6*, 31–40. [CrossRef]

25. Rivera, C. Essentials of Oral Cancer. *Int. J. Clin. Exp. Pathol.* **2015**, *8*, 11884.

26. Dzebo, S.; Mahmutovic, J.; Erkocevic, H. Quality of Life of Patients with Oral Cavity Cancer. *Mater. Sociomed.* **2017**, *29*, 30–34. [CrossRef]

27. Thavarool, S.B.; Muttath, G.; Nayanar, S.; Duraisamy, K.; Bhat, P.; Shringarpure, K.; Nayak, P.; Tripathy, J.P.; Thaddeus, A.; Philip, S.; et al. Improved Survival among Oral Cancer Patients: Findings from a Retrospective Study at a Tertiary Care Cancer Centre in Rural Kerala, India. *World J. Surg. Oncol.* **2019**, *17*, 15. [CrossRef]

28. Shrestha, A.D.; Vedsted, P.; Kallestrup, P.; Neupane, D. Prevalence and Incidence of Oral Cancer in Low- and Middle-Income Countries: A Scoping Review. *Eur. J. Cancer Care* **2020**, *29*, e13207. [CrossRef]

29. Leverrier, S.; Bergamaschi, D.; Ghali, L.; Ola, A.; Warnes, G.; Akgül, B.; Blight, K.; García-Escudero, R.; Penna, A.; Eddaoudi, A.; et al. Role of HPV E6 Proteins in Preventing UVB-Induced Release of pro-Apoptotic Factors from the Mitochondria. *Apoptosis* **2007**, *12*, 549–560. [CrossRef]

30. Eidet, J.R.; Pasovic, L.; Maria, R.; Jackson, C.J.; Utheim, T.P. Objective Assessment of Changes in Nuclear Morphology and Cell Distribution Following Induction of Apoptosis. *Diagn. Pathol.* **2014**, *9*, 92. [CrossRef]

31. Parikh, R.; Sorek, E.; Parikh, S.; Michael, K.; Bikovski, L.; Tshori, S.; Shefer, G.; Mingelgreen, S.; Zornitzki, T.; Knobler, H.; et al. Skin Exposure to UVB Light Induces a Skin-Brain-Gonad Axis and Sexual Behavior. *Cell Rep.* **2021**, *36*, 109579. [CrossRef]

32. Pfeifer, G.P. Mechanisms of UV-Induced Mutations and Skin Cancer. *Genome Instab. Dis.* **2020**, *1*, 99–113. [CrossRef]

33. Cuomo, R.E.; Mohr, S.B.; Gorham, E.D.; Garland, C.F. What Is the Relationship between Ultraviolet B and Global Incidence Rates of Colorectal Cancer? *Dermato-Endocrinol.* **2013**, *5*, 181–185. [CrossRef]

34. Ibbotson, S.H. A Perspective on the Use of NB-UVB Phototherapy vs. PUVA Photochemotherapy. *Front. Med.* **2018**, *5*, 184. [CrossRef]

35. Young, A.R.; Morgan, K.A.; Harrison, G.I.; Lawrence, K.P.; Petersen, B.; Wulf, H.C.; Philipsen, P.A. A Revised Action Spectrum for Vitamin D Synthesis by Suberythemal UV Radiation Exposure in Humans in Vivo. *Proc. Natl. Acad. Sci. USA* **2021**, *118*, e2015867118. [CrossRef]

36. Panov, V.; Borisova-Papancheva, T. Application of Ultraviolet Light (UV) in Dental Medicdine. *J. Med. Dent. Pract.* **2015**, *2*, 194–200. [CrossRef]

37. Agrawal, A.; Shindell, E.; Jordan, F.; Baeva, L.; Pfefer, J.; Godar, D.E. UV Radiation Increases Carcinogenic Risks for Oral Tissues Compared to Skin. *Photochem. Photobiol.* **2013**, *89*, 1193–1198. [CrossRef]

38. Salucci, S.; Burattini, S.; Battistelli, M.; Baldassarri, V.; Maltarello, M.C.; Falcieri, E. Ultraviolet B (UVB) Irradiation-Induced Apoptosis in Various Cell Lineages In Vitro. *Int. J. Mol. Sci.* **2013**, *14*, 532–546. [CrossRef]

39. Khalil, C. In Vitro UVB Induced Cellular Damage Assessment Using Primary Human Skin Derived Fibroblasts. *MOJ Toxicol.* **2015**, *1*, 138–143. [CrossRef]

40. Fernandez, T.L.; Van Lonkhuyzen, D.R.; Dawson, R.A.; Kimlin, M.G.; Upton, Z. In Vitro Investigations on the Effect of Dermal Fibroblasts on Keratinocyte Responses to Ultraviolet B Radiation. *Photochem. Photobiol.* **2014**, *90*, 1332–1339. [CrossRef]

41. Khalil, C. Combining Three In Vitro Assays for Detecting Early Signs of UVB Cytotoxicity in Cultured Human Skin Fibroblasts. *WIT Trans. Biomed. Health* **2006**, *10*, 349–359. [CrossRef]

42. Khalil, C.; Shebaby, W. UVB Damage Onset and Progression 24 h Post Exposure in Human-Derived Skin Cells. *Toxicol. Rep.* **2017**, *4*, 441–449. [CrossRef]

43. Boza, Y.; Yefi, R.; Rudolph, M.I.; Smith, P.C.; Oberyszyn, T.M.; Tober, K.L.; Rojas, I.G. Single Exposure of Human Oral Mucosa Fibroblasts to Ultraviolet B Radiation Reduces Proliferation and Induces COX-2 Expression and Activation. *Rev. Clínica De Periodoncia Implantol. Y Rehabil. Oral* **2010**, *3*, 123–127. [CrossRef]

44. Straface, E.; Vona, R.; Ascione, B.; Matarrese, P.; Strudthoff, T.; Franconi, F.; Malorni, W. Single Exposure of Human Fibroblasts (WI-38) to a Sub-Cytotoxic Dose of UVB Induces Premature Senescence. *FEBS Lett.* **2007**, *581*, 4342–4348. [CrossRef]

45. Chainiaux, F.; Magalhaes, J.-P.; Eliaers, F.; Remacle, J.; Toussaint, O. UVB-Induced Premature Senescence of Human Diploid Skin Fibroblasts. *Int. J. Biochem. Cell Biol.* **2002**, *34*, 1331–1339. [CrossRef]

46. Cavinato, M.; Koziel, R.; Romani, N.; Weinmüllner, R.; Jenewein, B.; Hermann, M.; Dubrac, S.; Ratzinger, G.; Grillari, J.; Schmuth, M.; et al. UVB-Induced Senescence of Human Dermal Fibroblasts Involves Impairment of Proteasome and Enhanced Autophagic Activity. *J. Gerontol. Ser. A* **2017**, *72*, 632–639. [CrossRef]

47. Kimura, H.; Lee, C.; Hayashi, K.; Yamauchi, K.; Yamamoto, N.; Tsuchiya, H.; Tomita, K.; Bouvet, M.; Hoffman, R.M. UV Light Killing Efficacy of Fluorescent Protein-Expressing Cancer Cells In Vitro and In Vivo. *J. Cell. Biochem.* **2010**, *110*, 1439–1446. [CrossRef]

48. Granados-López, A.J.; Manzanares-Acuña, E.; López-Hernández, Y.; Castañeda-Delgado, J.E.; Fraire-Soto, I.; Reyes-Estrada, C.A.; Gutiérrez-Hernández, R.; López, J.A. UVB Inhibits Proliferation, Cell Cycle and Induces Apoptosis via P53, E2F1 and Microtubules System in Cervical Cancer Cell Lines. *Int. J. Mol. Sci.* **2021**, *22*, 5197. [CrossRef]

49. Wang, H.-M.; Yang, H.-L.; Thiyagarajan, V.; Huang, T.-H.; Huang, P.-J.; Chen, S.-C.; Liu, J.-Y.; Hsu, L.-S.; Chang, H.-W.; Hseu, Y.-C. Coenzyme Q(0) Enhances Ultraviolet B-Induced Apoptosis in Human Estrogen Receptor-Positive Breast (MCF-7) Cancer Cells. *Integr. Cancer Ther.* **2017**, *16*, 385–396. [CrossRef]

50. Sarkar, S.; Rajput, S.; Tripathi, A.K.; Mandal, M. Targeted Therapy against EGFR and VEGFR Using ZD6474 Enhances the Therapeutic Potential of UV-B Phototherapy in Breast Cancer Cells. *Mol. Cancer* **2013**, *12*, 122. [CrossRef]

51. Bottone, M.G.; Santin, G.; Aredia, F.; Bernocchi, G.; Pellicciari, C.; Scovassi, A.I. Morphological Features of Organelles during Apoptosis: An Overview. *Cells* **2013**, *2*, 294–305. [CrossRef]

52. Bortner, C.D.; Cidlowski, J.A. Uncoupling Cell Shrinkage from Apoptosis Reveals That Na+ Influx Is Required for Volume Loss during Programmed Cell Death*. *J. Biol. Chem.* **2003**, *278*, 39176–39184. [CrossRef]

53. Doonan, F.; Cotter, T.G. Morphological Assessment of Apoptosis. *Methods* **2008**, *44*, 200–204. [CrossRef]

54. González-Juanatey, J.R.; Piñeiro, R.; Iglesias, M.J.; Gualillo, O.; Kelly, P.A.; Diéguez, C.; Lago, F. GH Prevents Apostosis in Cardiomyocytes Cultured In Vitro through a Calcineurin-Dependent Mechanism. *J. Endocrinol.* **2004**, *180*, 325–335. [CrossRef]

55. Toné, S.; Sugimoto, K.; Tanda, K.; Suda, T.; Uehira, K.; Kanouchi, H.; Samejima, K.; Minatogawa, Y.; Earnshaw, W.C. Three Distinct Stages of Apoptotic Nuclear Condensation Revealed by Time-Lapse Imaging, Biochemical and Electron Microscopy Analysis of Cell-Free Apoptosis. *Exp. Cell Res.* **2007**, *313*, 3635–3644. [CrossRef]

56. Chen, Q.; Kang, J.; Fu, C. The Independence of and Associations among Apoptosis, Autophagy, and Necrosis. *Signal. Transduct. Target. Ther.* **2018**, *3*, 18. [CrossRef]

57. Lindenboim, L.; Zohar, H.; Worman, H.J.; Stein, R. The Nuclear Envelope: Target and Mediator of the Apoptotic Process. *Cell Death Discov.* **2020**, *6*, 29. [CrossRef]

58. Ziegler, U.; Groscurth, P. Morphological Features of Cell Death. *News Physiol. Sci.* **2004**, *19*, 124–128. [CrossRef]

59. Povea-Cabello, S.; Oropesa-Ávila, M.; de la Cruz-Ojeda, P.; Villanueva-Paz, M.; De La Mata, M.; Suárez-Rivero, J.M.; Álvarez-Córdoba, M.; Villalón-García, I.; Cotán, D.; Ybot-González, P.; et al. Dynamic Reorganization of the Cytoskeleton during Apoptosis: The Two Coffins Hypothesis. *Int. J. Mol. Sci.* **2017**, *18*, 2393. [CrossRef]

60. Chipuk, J.E.; Bouchier-Hayes, L.; Green, D.R. Mitochondrial Outer Membrane Permeabilization during Apoptosis: The Innocent Bystander Scenario. *Cell Death Differ.* **2006**, *13*, 1396–1402. [CrossRef]

61. Lee, C.-H.; Yu, C.-L.; Liao, W.-T.; Kao, Y.-H.; Chai, C.-Y.; Chen, G.-S.; Yu, H.-S. Effects and Interactions of Low Doses of Arsenic and UVB on Keratinocyte Apoptosis. *Chem. Res. Toxicol.* **2004**, *17*, 1199–1205. [CrossRef]

62. Trabosh, V.A.; Daher, A.; Divito, K.A.; Amin, K.; Simbulan-Rosenthal, C.M.; Rosenthal, D.S. UVB Upregulates the Bax Promoter in Immortalized Human Keratinocytes via ROS Induction of Id3. *Exp. Dermatol.* **2009**, *18*, 387–395. [CrossRef]

63. Kim, Y.G.; Kim, H.J.; Kim, D.S.; Kim, S.D.; Han, W.S.; Kim, K.H.; Chung, J.H.; Park, K.C. Up-Regulation and Redistribution of Bax in Ultraviolet B-Irradiated Melanocytes. *Pigment. Cell Res.* **2000**, *13*, 352–357. [CrossRef]

64. Caricchio, R.; McPhie, L.; Cohen, P.L. Ultraviolet B Radiation-Induced Cell Death: Critical Role of Ultraviolet Dose in Inflammation and Lupus Autoantigen Redistribution 1. *J. Immunol.* **2003**, *171*, 5778–5786. [CrossRef]

65. Wu, Y.; Xing, D.; Liu, L.; Gao, B. Regulation of Bax Activation and Apoptotic Response to UV Irradiation by P53 Transcription-Dependent and -Independent Pathways. *Cancer Lett.* **2008**, *271*, 231–239. [CrossRef]

66. Qian, S.; Wei, Z.; Yang, W.; Huang, J.; Yang, Y.; Wang, J. The Role of BCL-2 Family Proteins in Regulating Apoptosis and Cancer Therapy. *Front. Oncol.* **2022**, *12*, 985363. [CrossRef]

67. Westphal, D.; Dewson, G.; Czabotar, P.E.; Kluck, R.M. Molecular Biology of Bax and Bak Activation and Action. *Biochim. Biophys. Acta. Mol. Cell Res.* **2011**, *1813*, 521–531. [CrossRef]

68. Ola, M.S.; Nawaz, M.; Ahsan, H. Role of Bcl-2 Family Proteins and Caspases in the Regulation of Apoptosis. *Mol. Cell. Biochem.* **2011**, *351*, 41–58. [CrossRef]

69. Shi, Y. Caspase Activation, Inhibition, and Reactivation: A Mechanistic View. *Protein Sci.* **2004**, *13*, 1979–1987. [CrossRef]

70. McIlwain, D.R.; Berger, T.; Mak, T.W. Caspase Functions in Cell Death and Disease. *Cold Spring Harb. Perspect. Biol.* **2013**, *5*, a008656. [CrossRef]

71. Eskandari, E.; Eaves, C.J. Paradoxical Roles of Caspase-3 in Regulating Cell Survival, Proliferation, and Tumorigenesis. *J. Cell Biol.* **2022**, *221*, e202201159. [CrossRef]

72. Miret, S.; De Groene, E.M.; Klaffke, W. Comparison of In Vitro Assays of Cellular Toxicity in the Human Hepatic Cell Line HepG2. *J. Biomol. Screen.* **2006**, *11*, 184–193. [CrossRef]

73. Cavalcante, G.C.; Schaan, A.P.; Cabral, G.F.; Santana-Da-Silva, M.N.; Pinto, P.; Vidal, A.F.; Ribeiro-Dos-Santos, Â. A Cell's Fate: An Overview of the Molecular Biology and Genetics of Apoptosis. *Int. J. Mol. Sci.* **2019**, *20*, 4133. [CrossRef]

74. Daher, A.; Simbulan-Rosenthal, C.M.; Rosenthal, D.S. Apoptosis Induced by Ultraviolet B in HPV-Immortalized Human Keratinocytes Requires Caspase-9 and Is Death Receptor Independent. *Exp. Dermatol.* **2006**, *15*, 23–34. [CrossRef]

75. Dunkern, T.R.; Fritz, G.; Kaina, B. Ultraviolet Light-Induced DNA Damage Triggers Apoptosis in Nucleotide Excision Repair-Deficient Cells via Bcl-2 Decline and Caspase-3/-8 Activation. *Oncogene* **2001**, *20*, 6026–6038. [CrossRef]

76. Park, Y.-K.; Jang, B.-C. UVB-Induced Anti-Survival and pro-Apoptotic Effects on HaCaT Human Keratinocytes via Caspase- and PKC-Dependent Downregulation of PKB, HIAP-1, Mcl-1, XIAP and ER Stress. *Int. J. Mol. Med.* **2014**, *33*, 695–702. [CrossRef]

77. Xu, H.; Yan, Y.; Li, L.; Peng, S.; Qu, T.; Wang, B. Ultraviolet B-Induced Apoptosis of Human Skin Fibroblasts Involves Activation of Caspase-8 and -3 with Increased Expression of Vimentin. *Photodermatol. Photoimmunol. Photomed.* **2010**, *26*, 198–204. [CrossRef]
78. Takasawa, R.; Nakamura, H.; Mori, T.; Tanuma, S. Differential Apoptotic Pathways in Human Keratinocyte HaCaT Cells Exposed to UVB and UVC. *Apoptosis* **2005**, *10*, 1121–1130. [CrossRef]
79. Brentnall, M.; Rodriguez-Menocal, L.; De Guevara, R.L.; Cepero, E.; Boise, L.H. Caspase-9, Caspase-3 and Caspase-7 Have Distinct Roles during Intrinsic Apoptosis. *BMC Cell Biol.* **2013**, *14*, 32. [CrossRef]